Real-Time Gait Analysis Using a Single Head-Worn Inertial Measurement Unit

Tong-Hun Hwang, *Student Member, IEEE,* Julia Reh, Alfred O. Effenberg, and Holger Blume, *Senior Member, IEEE*

***Abstract*—The background of our study is to apply advanced real-time gait analysis to walking interventions in daily-life setting. A vast of wearable devices provide gait information but not more than pedometer functions such as step counting, displacement and velocity. This paper suggests a real-time gait analysis method based on a head-worn inertial measurement unit (H-IMU). A novel analysis method implements real-time detection of gait events (heel strike, toe off, mid stance phase) and immediately provides detailed spatiotemporal parameters. The reliability of this method was proven by a measurement with over 11000 steps from seven participants on a 400 m outdoor track. The advanced gait analysis was conducted without any limitation of a fixed reference frame (e.g., indoor stage, infrared cameras). The mean absolute error in step-counting was 0.24%. Compared to a pedometer, additional gait parameters were obtained such as foot-ground contact time (CT) and contact time ratio (CTR). The gait monitoring system can be used as real-time and long-term feedback, which is applicable in the management of the health status and on injury prevention.**

***Index Terms*—Biomedical monitoring, Gait analysis, Inertial measurement unit, Smart devices, Wearable sensors**

I. Introduction

GAIT analysis is a key feature in consumer health monitoring. The number of steps can inform consumers of the amount of daily activity and calorie consumption. Gait speed is regarded as a vital sign, such as temperature, blood pressure and heart-beat rate [1], because of the strong correlation between the gait speed and seniors' motility [2]. In addition, information of gait balance can contribute to injury prevention. For example, monitoring gait balance control can aid the fall prevention of seniors [3] and the management of post-concussion [4]. Foot-ground contact time (CT) can be used for the rehabilitation after hip replacement [5]. Gait stride time variability was suggested as a predictor of overuse injuries during loaded and strenuous walking, which can aid the injury prevention in military training [6]. Therefore, people can benefit from the gait monitoring systems, in terms of the management of the health status and the prevention of injuries.

In the global market today, smartphones, wearable devices and internet of things (IoT) systems can provide gait analysis [7–10]. The gait monitoring units can even detect a pathologic gait [8, 9], and predict fall injuries [10]. Although most of healthcare wearable devices fail to sustain long-term engagement for users [11], pedometers have been continuously investigated to promote the sustainability of impact for the elderly [12] and the young [13, 14]. Interventions that encourages more walking benefit from pedometers because of the management of habitual activity and daily motivations [12–14]. Furthermore, wireless earphones have already been developed as a commercial health monitoring device [15]. The user friendliness and simplicity allows a seamless experience of the healthcare devices in everyday life. Virtual and augmented reality systems can support navigation applications with spatiotemporal gait parameters. A greater number of devices with head-worn sensors are expected to emerge in the healthcare industry.

This study demonstrates that the head-worn sensors can provide not only step counting like a pedometer, but also more spatiotemporal gait parameters that are strongly related to the health status. The proposed gait analysis system runs in real-time, using a wireless head-worn inertial measurement unit (H-IMU). The heel strike (HS), toe off (TO), and mid-stance phase are separately detected, thereby allowing the estimation of gait parameters, such as CT and a stride time. The experiment was conducted outdoors to demonstrate the applicability on daily life settings. In the next section, the previous work is discussed. Then, biomechanical terminologies of a gait cycle (the third section) and the proposed method for the gait event detection (the fourth section) are explained. Additionally, the estimation of gait parameters appears in the fifth section. Computations based on the measured data are introduced in the sixth section, followed by the conclusion.

II. Previous Works

A. Previous Systems in Gait Analysis

Reportedly gait analysis started with Aristotle thousands

This work was supported in part by European Commission HORIZON2020-FETPROACT-2014 No. 641321.

T.-H. Hwang is with the Institute of Sports Science and with the Institute of Microelectronic Systems, Leibniz University Hannover, 30167 Hannover, Germany (e-mail: tonghun.hwang@sportwiss.uni-hannover.de).

J. Reh is with the Institute of Sports Science, Leibniz University Hannover, 30167 Hannover, Germany (e-mail: julia.reh@sportwiss.uni-hannover.de).

A. O. Effenberg is with the Institute of Sports Science, Leibniz University Hannover, 30167 Hannover, Germany (e-mail: effenberg@sportwiss.uni-hannover.de).

H. Blume is with the Institute of Microelectronic Systems, Leibniz University Hannover, 30167 Hannover, Germany (e-mail: holger.blume@ims.uni-hannover.de).

years ago [16]. A couple of centuries ago, modern technologies (e.g., electrophysiology, photography) made innovation in measurement of human movement and gait analysis [16]. For kinetic analysis, pressure sensors can localize the feet and measure their forces [17]. Muscle kinetics is also analyzed with electromyography (EMG) [18]. For kinematic analysis, video analysis has been implemented [19]. Growing with film industry, 3 dimensional (3-D) motion capture technology has so far matured to be applied to gait analysis [20] by recording comprehensive kinematic information in 3-D space with sufficient precision to support gait analysis in different facets and even for highly demanding purposes as for stroke rehabilitation [21, 22].

B. Previous Motion Capture Systems

Motion capture systems include optical, non-optical and marker-less systems. Optical motion capture systems need cameras, markers and the source of optical waves in a certain range of spectrum, such as visible light and infrared ray (IR) [23]. Surrounding an actor, cameras detect optical wave reflected by markers on a suit which the actor is wearing. Referring to position information of markers, software regenerates the actor's movement in 3-D space. Although it is matured in 3-D animation movies and computer game industry, optical motion capture systems have errors from hidden markers which are placed behind human body from the view of cameras [24]. The use of multiple cameras also causes higher costs. Non-optical motion capture systems use inertial sensors [25], mechanical sensors or magnetic field. The inertial sensors generate kinematic information using inertial parameters such as acceleration, angular velocity, whereas mechanical sensors use banding angles of wires. In terms of magnetic marker systems, level of magnetic field near agents is used. From those parameters, systems finally obtain the body segment position or joint angle information. However, this technology also needs error compensation. For example, inertial motion capture systems show error accumulation in position data caused by double integration of accelerometer data, which is called drift effect. Mechanical motion capture systems lead to a limitation of motion because of wires and apparatus. Magnetic motion capture systems suffer from magnetic distortion from metal and electrical devices. In terms of marker-less systems, they animate motions without markers or sensors, which is a vision-based solution [26]. Using dual vision technology, two cameras can get image depth information. It is a handy system with a small number of devices and easy to use at home and therefore it is very popular in the computer game industry. Cameras, however, cannot see behind the body just like optical motion capture, and in addition they have much more hidden area so that it is called a 2.5-D motion capture system.

The inertial measurement unit (IMU) is used in this study. The accuracy of the inertial sensor units is significantly improved because of cutting edge microelectromechanical systems (MEMS) technology and sensor fusion with magnetometer [27], global positioning system (GPS) [28], or camera [29]. The IMU based on a combination of magnetometers and inertial sensors (accelerometer, gyroscope) can reduce drift effects of inertial sensors. Unlike optical motion capture systems, motion capture using an IMU system is implemented without fixed reference frames such as stages and cameras. This allows the measurement of human motion indoors [30] and outdoors [25]. Therefore, with advantages, IMU technology has quickly grown in gait analysis as well as in entertainment, education and sports industry.

C. Sensor Placement and Reduced Number of Sensors

Researchers explorer optimal positions to analyze gait by using a much smaller number of sensors than the whole body solution. They tested these simpler systems by using foot switches or inertial sensors which were fixed onto the foot, the tibia, the thigh, and the pelvis [31]. They successfully analyzed gait events, knee angle and foot orientation. Real time analysis was, however, implemented only when including foot switchers in its sensor combination, which are impractical in daily life. They also conducted the experiments by using wired devices in laboratories and clinics, conditions all together, quite far away from everyday life conditions. Nevertheless, it was shown that a smart phone can perform walking detection and counting steps, even placed in a hand, a backpack, a handback, and trouser pockets [7]. This demonstrated that a single sensor unit can be applied in gait event detection, independently from its placement.

D. Previous Work Using Head-Worn Sensor

A head-worn sensor has been implemented to research on head stability during walking [32–34]. Researchers have analyzed head accelerations to assess coordination with the neck and the truck on three axes [32]. They found that head accelerations have reliably regular patterns related to gait. Although acceleration signals were attenuated due to stabilizing effect of the neck and the trunk [32–34], researchers have referred to the head in analyzing gait patterns [35]. A wireless ear-worn sensor was demonstrated for the gait pattern analysis, which allowed to recognize pathologic gait [9]. The ear-worn sensor can also detect HS in real time. However, it includes several cycle delay, and needs a combination with a pressure sensing platform in order to deliver the advanced gait information [36]. Finally, it was reported that an H-IMU alone can detect TO as well as HS in real time, thereby allowing the measurement of detailed gait parameters (e.g., CT, stride length) [30]. It was conducted in the laboratory but not in an outdoor setting shown in this paper.

III. GAIT CYCLE

A gait cycle is defined as a specific sequence of repetitive events during walking. The gait cycle consists of stance phase and swing phase, which are divided by two gait events, HS and TO. Stance phase is a time period when the foot contacts the ground and the leg supports the body. Swing phase is another time period when the foot swings and moves forward. Heel strike is the end point of the swing phase and the beginning of the stance phase, whereas TO is the end of the stance phase and

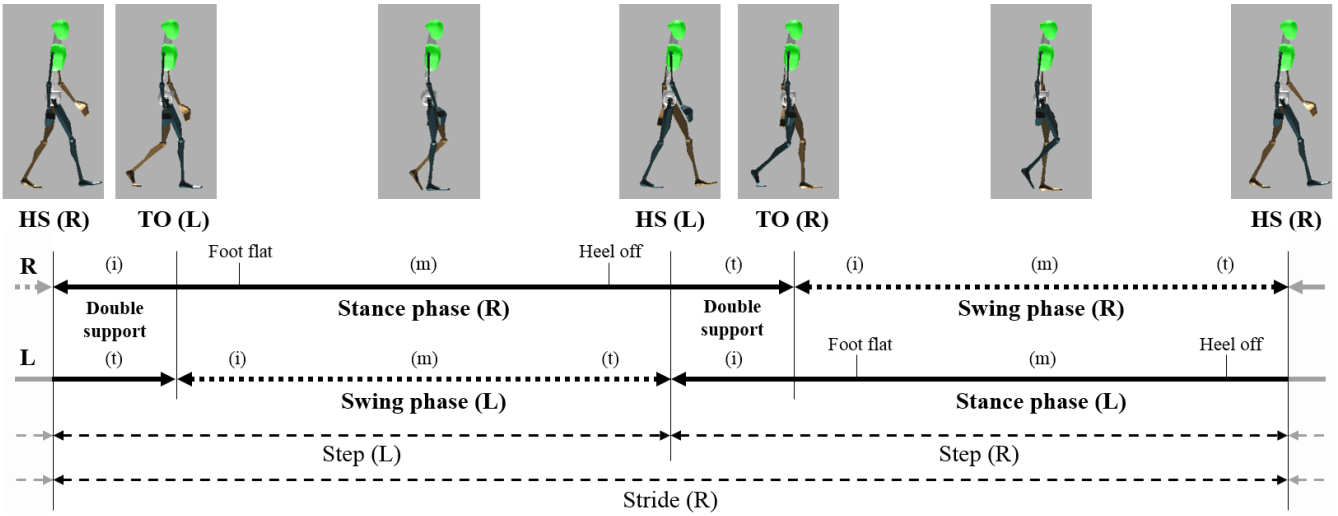

Fig. 1. Time diagram of a gait cycle with example pictures at walking gait events which are from the right side view along the sagittal axis. Abbreviations of 'HS' is heel strike, 'TO' is toe off, 'R' is right, 'L' is left, (i) is initial phase, (m) is mid-phase, and (t) is terminal phase.

the beginning of the swing phase. The time points of phases and events are important in measuring spatiotemporal gait parameters.

In Fig. 1, a gait cycle is shown with exemplary walking motions and its time diagram. The walking motions are from the right side view on the sagittal plane. In the time diagram of Fig. 1, phases and events are described. The walking cycle starts with a right HS, which is the initial point of the right stance phase. It is followed by a left TO, that finishes the left stance phase and starts the left swing phase. The right foot lies flat on the ground (i.e., foot flat) and the mid-stance phase starts, while the left foot is in the mid-swing phase. Subsequently, it changes from the right stance phase to the terminal stance phase and the right heel off occurs. This is followed by the left HS whereby the left stance phase starts. Thus, this phase can be described as a double support period. The duration from right HS to left HS is defined as left step time. After the left HS, another step starts in the same order as described before, but the foot has changed (right step). At the end of the right stance phase the right TO occurs, which finishes the right CT. This is the period between the right HS and the right TO, which is a step time plus a double support time. The contact time depends on gait velocity but is approximately 60% of the stride time. The ratio between the contact time to the stride time is called ground contact time ratio (CTR). Left foot flat, left heel off, and the right HS are followed as a sequence. The duration from left HS to right HS is the right step time. This complete sequence is one gait cycle and also named a stride time, which is repeated during walking.

IV. Methodology of Gait Detection Using H-IMU

Gait analysis using a single H-IMU was implemented with an IMU system which included a 3-D accelerometer, a 3-D gyroscope, and a 3-D magnetometer. This sensor combination can generate accurate kinematic data by minimizing error accumulation. The system regenerates zero-gravity acceleration to detect the impact of the feet. Vertical acceleration of the head is processed for peak detection because the impact on the foot at HS and TO is transmitted to the head along longitudinal body axis, which is identical to the z-axis of the head (see Fig. 4(a)). The peak detection algorithm finds peaks in the vertical acceleration at HS and TO. A thresholding algorithm eliminates the small peaks which are unwanted signals. For instance, peaks occur when the head sways, nods, and direct the line of sight from one place to another place during walking. White noise also makes small peaks. A digital filter reduces noise and makes the signal smooth, in order to improve estimation of kinematic parameters and spatiotemporal accuracy in gait event detection.

A. Peak Detection

Peak detection is one of the most accurate methods in gait event detection [7]. It can be implemented on the pelvis, the hip, the thigh, the tibia, and the feet [8]. For the single sensor solution, it can be realized on the waist and the wrists, as well as in the backpack and the handbag [7]. The peak is detected by comparison of the derivative before and after a sample point of interest. When the signs of these derivatives are different, the sample point is a peak. Generally, peaks appear in sensor signals over time, so that peaks at gait events must be distinguished from irrelevant peaks. At gait events, peaks show characteristics which differ depending on the considered body part.

In Fig. 2, vertical (z-axis) accelerations of four body parts are shown. From the top, the left foot, the right foot, the pelvis, and the head are arranged in order. Each body part has different clues at HS and TO. Considering foot acceleration, the highest peak occurs, which is defined as an HS. A stance phase which keeps a certain level of acceleration without fluctuation follows, and then several peaks occur again. The last negative peak is regarded as TO before an abrupt drop in acceleration. In terms of pelvic acceleration, the first high peak is assumed as HS and the negative peak before the second peak is regarded as TO. For head acceleration, the first high peak is defined as HS. From the HS, the third peak is regarded as TO.

In the foot acceleration in Fig. 2, the highest peaks are over 30 m/s^2 at HS and peaks at TO also reach around 10 m/s^2, which are easily distinguishable. However, other high peaks occur

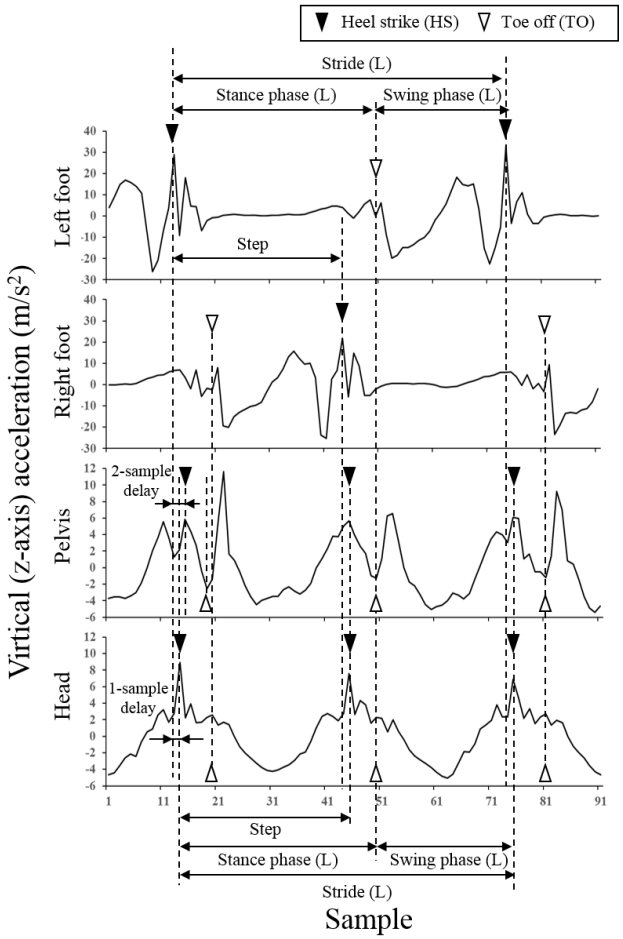

Fig. 2. Vertical acceleration of body segments of the left foot, the right foot, the pelvis and the head which are measured at 60 Hz.

near the peaks at HS and TO as well as during swing phase, which reduces accuracy of gait event detection. In addition, a foot sensor can aid gait event detection for only one foot, whereas a sensor fixed onto the pelvis or the head can detect gait events of both feet as shown in Fig. 2. Peak detection with the head acceleration has more advantages than the pelvic acceleration [30]. Compared to pelvic acceleration, head acceleration shows clearly outstanding peaks. Pelvic acceleration shows two high peaks at HS and TO, thereby causing a confusion in analysis. Head peak acceleration has less delay from foot peak acceleration than pelvic acceleration as shown in Fig. 2.

B. Thresholding

Gait event detection needs thresholding to determine if peaks occur due to gait events or noise. The threshold value has to be changed depending on gait velocity. This is because an increased gait velocity generally results in higher peak acceleration at gait events but also in higher noisy peak acceleration. To be specific, a higher threshold properly works for a higher gait velocity because the impacts at gait events generate higher peak acceleration. In contrast, a lower threshold is suitable for slower gait, because the peaks are smaller. The level of threshold value can be empirically decided.

Thresholding method is more effective for head acceleration than for the other two parts in Fig. 2. The head acceleration shows clearly outstanding peaks at HS, whereas noisy peaks occur near to HS, TO and the swing phase in foot and pelvic acceleration, which causes confusion in setting optimal thresholds and increases errors in gait event detection. For head acceleration, however, it is easier to find an optimal threshold because of less confusing peaks near HS and TO.

C. Digital Filter

To improve the quality of data, an IMU system needs digital filters which can reduce noise and eliminate unwanted signals [37, 38]. In gait analysis, well-designed digital filters can reduce errors of gait parameters such as step length, displacement, cadence and the number of steps because of reliable sensor data. Digital filters are categorized into two classes, a finite impulse response (FIR) filter [37] and an infinite impulse response (IIR) filter [38]. Finite impulse response filters modulate a finite number of inputs from the past to the present, which finally generates present output. High-, low- and band-pass filters as well as Gaussian and median filters are included in FIR filters which reduce white noise or unwanted signals. FIR filter helps in detecting peaks at gait events by smoothing unwanted peaks near gait events. On the other hand, IIR filters use an infinite number of inputs because of recursive function. This means the present output is a function of past outputs which are modulated from past inputs. The present output is, therefore, related by all past inputs as like a feedback loop. Kalman filter represents IIR filters and can reduce not only white noise, but also offset errors from sensors or systems. Kalman filter is designed from state equation based modeling, which is expressed by a set of differential equations. Kalman filters with IMU are broadly used in estimation of displacement in terms of aerospace, navigation and gait analysis [29]. Kalman filters are developed in different practices.

In time domain, convolution of FIR filters and input signals generate a filtered output signal. Convolution, however, takes Θ (N^2) of complexity. For faster algorithm, computer programs execute convolution in frequency domain after fast Fourier transform (FFT). In frequency domain, a convolution is just a multiplication and its complexity, thereby, decreases to Θ (N log N) the same as the complexity of FFT. After multiplication in frequency domain, inverse fast Fourier transform (IFFT) returns the data in time domain, which becomes a result of the convolution. Discrete wavelet transform (DWT) and inverse discrete wavelet transform (IDWT) can reduce unwanted frequency components. Thresholding in DWT also efficiently reduces noise, which takes the lowest complexity of Θ (N) [9]. With FFT/IFFT, however, more variations in filter design are allowed for different gait styles and gait velocities.

V. Gait Parameters with H-IMU

An H-IMU can provide head acceleration, which is used in gait event detection. Spatiotemporal gait parameters can be obtained from gait event detection. Head acceleration, velocity, and position show a specific pattern for human gait. From the patterns, the exact time points at gait events are detected. Spatiotemporal gait parameters are calculated from the position and the time point at HS and TO.

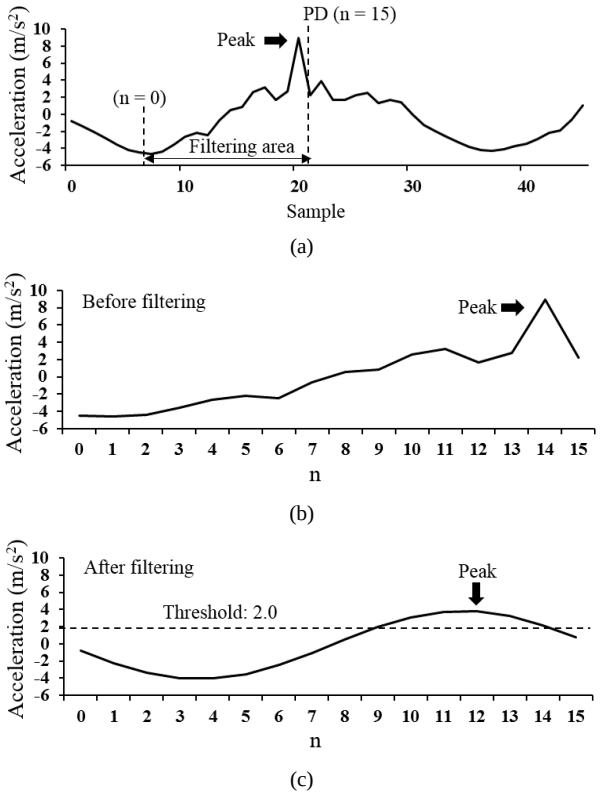

Fig. 3. Head vertical acceleration are shown (a) 46 samples near an HS depicted with filtering area, (b) with 16 samples before filtering, and (c) 16 samples after filtering, which are measured at 60 Hz so that intervals between samples are 16.7 ms.

A. Temporal gait parameters

Temporal gait parameters are obtained from time points of HS and TO. As shown in Fig. 2, a head-worn sensor can detect gait events of both the right and left foot, and the stance phase and the swing phase are calculated by the difference between the gait events.

When detecting HS, an FIR filter and thresholding are used as shown in Fig. 3. At HS, peaks on head acceleration is around 1-sample delayed from peaks on foot acceleration, which is around 16.7 ms delay at 60 Hz. An FIR filter can reduce the delay between head peak acceleration and foot peak acceleration. In addition, double peaks can appear at an HS because the second impact occurs at foot flat as strong as at HS; however, the FIR filter can change the double peaks to one peak by using smoothing effect, which helps in avoiding confusion in HS detection. An ideally selected threshold can also enhance the accuracy of gait event detection by reducing noise.

At TO, a foot pushes down the ground and starts hover in the air. In foot acceleration, a relatively high peak is observed because it is relative to the propulsion force which makes the body move forward. The force is transmitted to the head, which is observed as a peak on head acceleration. The peak is too small to be determined whether it is the peak at TO or not. However, the third peak is normally the time point of TO, following HS (the first peak) and foot flat (the second peak). In case TO is not found with the third peak of acceleration because of an exceptional acceleration pattern, the negative peak of head velocity is considered as TO. This avoids skipping TO detection.

The accurate time point of gait events provides accurate temporal parameters. The period of a stance phase is obtained from the time difference from an HS to the following TO of one foot, whereas the period of a swing phase is from a TO to the following HS of one foot. A step time is from an HS of a foot to the next HS of another foot. A stride time is from an HS of a foot to the next HS of the same foot. Cadence is defined as the number of steps per minute. To get cadence, first of all, the number of steps is measured by counting the number of HS. This is because the number of HS is the same as that of steps. HS detection is the easiest and the most accurate method. Second, travel duration is measured by a timer in IMU system. When the number of HS is divided by travel duration in minutes, cadence is obtained.

B. Spatial gait parameters

Spatial gait parameters include step length (SL), stride length, and travel distance. A single IMU has a global position in 3-D space, which includes the horizontal position of the head in x-y Cartesian coordinate system. From the positions, spatial gait parameters are obtained during walking as shown in Fig. 4.

Step length can be measured from the distance between an HS position of one foot to the following HS position of the other foot. The distance between two feet is measured along the walking direction, which means foot positions are measured after projected on the vector of walking direction as shown in Fig. 4. The head position, however, can provide the average SL. The distance between the head position at an HS and at the following HS is equivalent to the summation of the latter part of an SL and the former part of the next SL, which we call the pseudo step length (PSL) [26]. With $n = 1, 2, 3, \ldots$, the n-th step length, SL_n, is separated into two parts $SL_n.a$ and $SL_n.b$ as shown in (1). The n-th PSL is sum of $SL_n.b$ and $SL_{n+1}.a$ as shown in (2).

$$SL_n = SL_n.a + SL_n.b. \tag{1}$$

$$PSL_n = SL_n.b + SL_{n+1}.a. \tag{2}$$

From two equations, the relationship between the average of the SL and the PSL is defined as

$$\begin{aligned} \mathrm{E}[SL] &= \frac{1}{N}\sum_{k=1}^{N} SL_k = \frac{1}{N}(SL_1.a + \sum_{k=1}^{N-1} PSL_k + SL_N.b) \\ &= \frac{1}{N-1}\sum_{k=1}^{N-1} PSL_k + \frac{1}{N}(SL_1.a + SL_N.b - \frac{1}{N-1}\sum_{k=1}^{N-1} PSL_k) \\ &= \mathrm{E}[PSL] + \frac{1}{N}\{(SL_1.a + SL_N.b) - \mathrm{E}[PSL]\} \\ &= \mathrm{E}[PSL] + k \end{aligned} \tag{3}$$

where E is the expectation, N is the number of HS and k is a constant. As the number of HS increases, k is negligible so that E[SL] and E[PSL] are nearly the same. In addition, they have

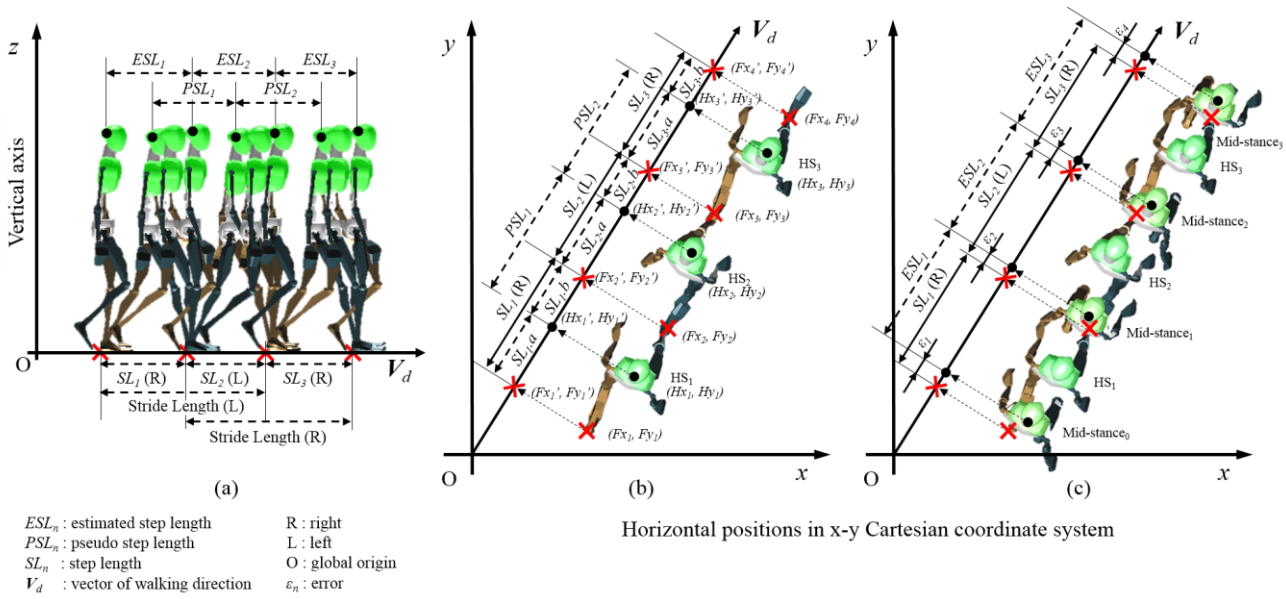

Fig. 4. The avatar shows (a) the side view of walking avatar depicted with SL, PSL and ESL methods, (b) the top view of walking avatar depicted with SL and PSL, and (c) the top view of walking avatar depicted with SL and ESL.

very close values when *SL* have the similar values in a regular gait velocity. If there are the *N+1* th *SL* and the *N* th *PSL*,

$$SL_1.a + SL_N.b \approx SL_{N+1}.a + SL_N.b = PSL_N \approx \mathrm{E}[PSL] \tag{4}$$

when all former parts, $SL_n.a$, are similar. In regular gait, one PSL_N and average *PSL* are similar as well. The constant *k* is finally close to 0 as shown below:

$$k = \frac{1}{N}\{(SL_1.a + SL_N.b) - \mathrm{E}[PSL]\} \approx 0. \tag{5}$$

For another estimation, the step length is measured from head positions at the mid-stance phase as shown in Fig.4(c). The positon of one foot can be measured when the head vertical position is the highest. This is because the head vertical positon reaches the peaks when the leg is straight and orthogonal against the ground. In the side view on the sagittal plane (Fig. 4(a)), the head is located directly above a foot, which is also depicted in the top view as shown in Fig. 4(c). The head position, therefore, can be used to estimate not only the foot position, but also the SL which we call the estimated step length (ESL). The equation of *n*-th step length, SL_n, and *n*-th estimated step length, ESL_n, is below:

$$SL_n = ESL_n + \varepsilon_n - \varepsilon_{n+1} = ESL_n + \xi_n \tag{6}$$

where n = 1, 2, 3, … and ε_n is the difference between head position and foot position at mid-stance phase. The error between SL_n and ESL_n is ξ_n. If the left and right step lengths are regularly different, the error of SL can be estimated from average right foot error, $\mathrm{E}[\varepsilon_{2n}]$, and average left foot error, $\mathrm{E}[\varepsilon_{2n-1}]$. Estimated error ε_E is defined as

$$\varepsilon_E = \mathrm{E}[\varepsilon_{2n-1}] - \mathrm{E}[\varepsilon_{2n}] \approx \xi_n. \tag{7}$$

From (6) and (7), there are two different equations for the left and the right step length as below:

$$\begin{aligned} SL_{2n-1} &\approx ESL_{2n-1} + \varepsilon_E. \\ SL_{2n} &\approx ESL_{2n} - \varepsilon_E \end{aligned} \tag{8}$$

where SL_{2n-1} and SL_{2n} are step lengths for the left and right foot and ESL_{2n-1} and ESL_{2n} are estimated step lengths for the left and right foot as well. With difference of even and odd SL, it is distinguishable which SL is from the right step or the left step. When it is the left-right balanced gait so that ε_n and ε_{n+1} show a small difference, SL_n and ESL_n are nearly the same.

The stride length can be calculated from the distance between an HS position of one foot and the following HS position of the same foot. The average stride length can be twice of the average step length. Left stride length starts with the left HS and ends with the next left HS, which is equivalent to the sum of right SL and left SL in the order. The right stride length is calculated by the sum of the left SL and right SL in the order. A stride length can be estimated from the sum of the right and the left ESL.

The travel distance can be obtained by double integration of acceleration or the sum of step lengths. Both methods can include an error from the trajectory of swayed head which makes more travel distance. It is, as a result, needed to project the trajectory onto the vector of gait direction.

VI. Results

Gait analysis was implemented using an H-IMU from a commercial IMU system which was already developed as hardware and software packages [39]. For hardware, seventeen IMUs and a wireless communication router (base frequency: 2.4 GHz) are included for the whole body motion capture system. The software renders 3-D biomechanical human models with the whole body system. The software solution

TABLE I
COMPARISON OF THREE METHODS IN STEP COUNTING

Participant (Age; year)	Manual count	Pedometer		H-IMU	
		Steps	SCER (%)	Steps	SCER (%)
M1 (30)	1105	1117	1.09	1100	-0.45
M2 (24)	1866	1851	-0.80	1857	-0.48
M3 (34)	1799	1801	0.11	1796	-0.17
F1 (30)	2699	2697	-0.07	2697	-0.07
F2 (35)	1221	1223	0.16	1221	-0.00
F3 (28)	1868	1866	-0.11	1862	-0.32
Total	10558	10555	-0.03	10533	-0.24
Mean absolute error		35	0.33	25	0.24

supports real-time measurement of acceleration, velocity, position, and orientation of IMUs. We carried out data analysis by using only head kinematic data. The analysis was implemented at a 60 Hz sampling rate.

A. Step counting

Step counting was implemented by head kinematic data provided by the H-IMU. Kinematic data of a physiological gait pattern were captured with six participants (3 males, 3 females; age: 30.2 ±3.7 years; height: 174.3 ±9.0 cm. A commercial pedometer placed on the waist was also used for comparison. For one trial, participants were asked to walk one round on the third lane of a 400 m track plus 25 m in the constant speed. They walked between two and four trials as participants' preference. Table I compares step counting from manual count, a pedometer, and an H-IMU. In total, 10558 steps are manually counted as a ground truth. The pedometer counted 10555 steps, whereas the H-IMU counted 10533 steps. The step counting error ratio (SCER) of the pedometer and H-IMU were -0.03% and -0.24%. Pedometer showed less SCER because it made errors with over and skip counting, whereas the H-IMU made errors with skip counting. Overall, the H-IMU made less mean absolute error as 25 steps than the pedometer's absolute error as 35 steps, which showed H-IMU was more accurate than the pedometer. The third male participant (M3) walked three trials by 1799 steps. Compared to other male participants, both the pedometer and the H-IMU showed accurate results as 1801 steps (0.11% SCER) and 1796 steps (-0.17% SCER). In terms of female participants, the first participant walked four trials with 2699 steps. Both devices more accurately counted steps as 2697 steps (-0.07% SCER) than other female participants. The participant M1 had less accuracy than other participants because they have high peak at TO, which made both measurement devices confused. The participant M2 walked fast so that pedometer might have skipped more steps. Participants M3 and F2 were older than others and steps were counted more accurately. Females' gait was also detected more accurately than males' gait. Although different participants have different gait style, the H-IMU provides data nearly close to the ground truth without changing digital filters and threshold values.

B. Analysis of spatiotemporal parameters

Temporal parameters of seven participants are shown in Table II. Including participant M4, participants' age was 29.6 ±3.7 years and height was 175.7 ±9.0 cm. Total 11112 steps were analyzed for gait parameter. Some parameters were calculated with sampled 10454 steps excluding the beginning and the end data because of instability. For participants M1 and M3, more data were excluded after one point at the middle because participants changed their speed abruptly, which is not constant speed. The participant M2 had the highest cadence as 124.4 steps per minute and the shortest CT as 579.8 ±26.4 ms. The participant F2, on the other hand, had lowest cadence as 106.8 steps per min and the longest CT as 676.6 ±33.7 ms. Other participants' cadences were between 112.9 and 117.6 steps per minute. Participant M4 had the highest CTR as 60.9%, whereas participant M1 had the lowest CTR as 60.0%.

For spatial gait parameters, the step length was measured with two methods, PSL and ESL. The PSL was generally higher than the ESL except for participant M1. Estimated step length showed larger standard deviation because it included difference values between left and right step length. From ESL, the participant M1 had the longest step length as 768.5 ±105.1 mm. The shortest step length was recorded by the participant F1 as 655.2 ±32.7 mm. Step length tends to correlate with height except for M2 and M4. For distance, participants walked along the third lane of the 400 m track. participants walked between the inside length of the third lane and the fourth lane, which is between 415.33 m and 423.0 m for one round according to international association of athletics federations (IAAF). For one trial, 25 m is added on the distance of one round. This means the minimum lengths from one trial to four trials are 440.33 m, 880.66 m, 1320.99 m, and 1761.32 m. When the error between the track length and the measurement result is 0.0

TABLE II
SPATIOTEMPORAL PARAMETERS COMPUTED BY H-IMU

Participant (Age; year)	Height (cm)	Sampled steps (Total steps)	Cadence (steps/min)	CT (ms) (Avg. ±Std.)	CTR (%)	PSL (mm) (Avg. ±Std.)	ESL (mm) (Avg. ±Std.)	Number of trials	Total Distance (m)	Distance error per trial[a] (m)
M1 (30)	190	893 (1110)	112.9	645.6 ±53.5	60.0	763.7 ±60.1	768.5 ±105.1	2	853.0	-13.8
M2 (24)	179	1836 (1857)	124.4	579.8 ±26.4	60.1	729.5 ±44.3	727.9 ±110.2	3	1351.7	10.2
M3 (34)	177	832 (1189)	117.4	616.6 ±34.0	60.3	754.4 ±42.6	754.2 ±67.3	2	896.7	-2.2
M4 (26)	184	1162 (1176)	109.5	667.6 ±28.5	60.9	715.2 ±57.5	713.6 ±54.8	2	839.2	-20.8
F1 (30)	162	2669 (2697)	117.6	618.1 ±20.1	60.6	658.4 ±25.7	655.2 ±32.7	4	1767.1	1.4
F2 (35)	170	1207 (1221)	106.8	676.6 ±33.7	60.2	720.9 ±61.9	717.6 ±51.1	2	876.2	-2.3
F3 (28)	168	1841 (1862)	113.0	644.5 ±26.3	60.7	686.6 ±49.0	684.1 ±79.8	3	1273.8	-15.7

[a]Distance error per trial is calculated based on distance differences from the inside length of the third lane on 400 m track plus 25 m (ground truth: 440.33 m).

m−7.67 m per trial, it might not be regarded as the measurement error. When the error is under 0.0 m or over 7.67 m, it might result from the measurement error, such as accumulation error of IMU systems. The total distance was obtained from multiplication of total steps and ESL. Participant M1 and M3 walked less than two trials so that they show approximate results. Their total distances for two trials were 853.0 m (M1) and 896.7 m (M3), which had -13.8 m (M1) and -2.2 m (M3) of errors per trial. Participants M4 and F2 walked two trials with 839.2 m and 876.2 m, which had -20.8 m and -2.3 m of errors per trial, respectively. Participant M2 and F3 walked three trials with 1351.7 m (M2) and 1273.8 m (F3), which had 10.2 m (M2) and -15.7 m (F3) of errors per trial. Participant F1 walked four trials with 1767.1 m, which 1.4 m error per trial.

VII. Conclusion

Compared to pedometers, the proposed method can provide a large number of spatiotemporal gait parameters (e.g., foot-ground contact time, contact time ratio, stride time) that are strongly related to the daily health status. By using software with mobile applications, this method can reach the mass market because most wearable devices have IMU sensors, at least accelerometers. The data of our system might be transformed into acoustic signals to pace Parkinson patients [40] and even might initiate multisensory learning effects [41]. Issues of health monitoring systems (e.g., security, battery life, sustainable engagement for users) should be solved in the future. Our study can, nevertheless, contribute to sustainability of engagement for end-users, providing a seamless experience and motivation for walking. For the future work, advanced analysis with H-IMU would be developed to cover various types of gait like running and jumping. With head gesture recognition, H-IMU can be used in future studies on human-human interactions in teacher-student and therapist-patient dyads in walking settings.

References

[1] S. Fritz, and M. Lusardi, "White paper:"walking speed: the sixth vital sign"," *J. geriatric physical therapy*, vol. 32, no. 2, pp. 2–5, 2009.

[2] S. Studenski, S. Perera, K. Patel, C. Rosano, K. Faulkner, M. Inzitari J. Brach, J. Chandler, P. Cauthon, E. B. Conner, and Nevitt, M, "Gait speed and survival in older adults," *Jama*, vol. 305, no. 1, pp. 50–58, 2011

[3] S. A. Bridenbaugh, and R. W. Kressig, "Laboratory review: the role of gait analysis in seniors' mobility and fall prevention," *Gerontology*, vol. 57, no. 3, pp. 256–264, 2011.

[4] D. Howell, L. Osternig, and L. S. Chou, "Monitoring recovery of gait balance control following concussion using an accelerometer," *J. biomechanics*, vol. *48*, *no. 12*, pp. 3364–3368, 2015.

[5] J. Reh, T.-H. Hwang, V. Michalke, and A. O. Effenberg, "Instruction and real-time sonification for gait rehabilitation after unilateral hip arthroplasty," in *11th joint Conf. Motor Control & Learning, Biomechanics & Training. dvs*, Damstadt, Germany, Sep. 28–30, 2016.

[6] S. Springer, U. Gottlieb, & M. Lozin, "Spatiotemporal Gait Parameters as Predictors of Lower-Limb Overuse Injuries in Military Training," *The Scientific World Journal*, 2016.

[7] A. Brajdic, and R. Harle, "Walk detection and step counting on unconstrained smartphones," in *Proc. the 2013 ACM Int. Joint Conf. Pervasive and Ubiquitous Computing*, Zurich, Switzerland, 2013, pp. 225–234.

[8] M. Yamada, T. Aoyama, S. Mori, S. Nishiguchi, K. Okamoto, T. Ito, S. Muto, T. Ishihara, H. Yoshitomi, and H. Ito, "Objective assessment of abnormal gait in patients with rheumatoid arthritis using a smartphone," *Rheumatology international*, vol. 32, no. 12, pp. 3869–3874, Dec. 2012.

[9] L. Atallah, O. Aziz, B. Lo, and G. Z. Yang, "Detecting walking gait impairment with an ear-worn sensor," In *IEEE 6th Int. Workshop on BSN 2009*, Berkeley, CA, 2009, pp. 175–180.

[10] A. J. A. Majumder, P. Saxena, and S. I. Ahamed, "Your walk is my command: gait detection on unconstrained smartphone using IoT system," in *Proc. IEEE 40th Annu. COMPSAC*, Atlanta, GA, 2016, pp. 798-806.

[11] Ledger D, Partners E, Scientist B, Manager P, "Inside Wearables: How the science of human behavior change offers the secret to long-term engagement," *Endevour Partners*, Jan. 2014. [Online]. Available: https://blog.endeavour.partners/

[12] T. Harris, S. M. Kerry, C. R. Victor, U. Ekelund, A. Woodcock, S. Iliffe, P. H. Whincup, C. Beighton, M. Ussher, E. S. Limb, L. David, D. Brewin, F. Adams, A. Rogers, D. G. Cook, "A primary care nurse-delivered walking intervention in older adults: PACE (pedometer accelerometer consultation evaluation)-Lift cluster randomised controlled trial," *PLoS medicine*, vol. 12, no. 2, 2015, DOI: 10.1371/journal.pmed.1001783.

[13] J. Inchley, L. Cuthbert, & M. Grimes, "An investigation of the use of pedometers to promote physical activity, and particularly walking, among school-aged children," CAHRU, Univ. Edinburgh, UK, 2007.

[14] J. A. Rye, S. J. Zizzi, E. A. Vitullo, and N. O. H. Tompkins, "The pedometer as a tool to enrich science learning in a public health context," *J. of Science Education and Tech.*, vol. 14, no. 5–6. pp. 521–531, 2005.

[15] N. Hunn, "The market for hearable devices 2016–2020," *Technical report November*, WiFore Consulting, London, UK, Nov. 2016.

[16] R. Baker, "The history of gait analysis before the advent of modern computers," *Gait & Posture*, vol. 26, no.3, pp. 331–342, Sep. 2007.

[17] J. Nilsson, V. P. Stokes, A. Thorstensson, "A new method to measure foot contact," *J. Biomechanics*, vol. 18, no. 8, pp. 625–627, 1985.

[18] A. Muro-De-La-Herran, B. Garcia-Zapirain, and A. Mendez-Zorrilla, "Gait analysis methods: An overview of wearable and non-wearable systems, highlighting clinical applications," *Sensors*, vol. 14, no. 2, pp. 3362–3394, 2014.

[19] R. B. Davis, S. Ounpuu, D. Tyburski, and J. R. Gage, "A gait analysis data collection and reduction technique," *Human Movement Sci.*, vol. 10, no. 5, pp. 575–587, 1991.

[20] A. Pfister, A. M. West, S. Bronner, and J. A. Noah, "Comparative abilities of Microsoft Kinect and Vicon 3D motion capture for gait analysis," *J. Med. Eng. Technol.*, *38(5)*, pp. 274–280, Mar. 2014, DOI: 10.3109/03091902.2014.909540.

[21] H. Brock, G. Schmitz, J. Baumann, and A. O. Effenberg, "If motion sounds: Movement sonification based on inertial sensor data," in *the Engineering of Sport Conf. 2012*, Lowell, Massachusetts, 2012, pp. 556–561, DOI: 10.1016/j.proeng.2012.04.095

[22] G. Schmitz, D. Kroeger, and A. O. Effenberg, "A mobile sonification system for stroke rehabilitation," in *The 20th Int. Conf. on Auditory Display*, New York, 2014.

[23] A. G. Kirk, J. F. O'Brien, and D. A. Forsyth, "Skeletal parameter estimation from optical motion capture data," in *IEEE-CS Conf. CVPR 2005*, San Diego, CA, 2005, vol. 2, pp. 782–788.

[24] M. C. Silaghi, R. Plänkers, R. Boulic, P. Fua, and D. Thalmann, "Local and global skeleton fitting techniques for optical motion capture," in *Proc. Int. Workshop CAPTECH98*, Geneva, Switzerland, 1998, pp. 26–40.

[25] M. Brodie, A. Walmsley, and W. Page, "Fusion motion capture: a prototype system using inertial measurement units and GPS for the biomechanical analysis of ski racing," *Sports Technol.*, vol. *1, no.1*, pp. 17–28, Jun. 2008.

[26] T. B. Moeslund, A. Hilton, and V. Krüger, "A survey of advances in vision-based human motion capture and analysis," *Computer Vision and Image Understanding*, vol. 104, no. 2, pp. 90–126, Nov. 2006.

[27] J. A. Rios, and E. White, "Fusion filter algorithm enhancements for a MEMS GPS/IMU," in *ION NTM 2002*, San Diego, CA, 2002, pp. 28-30.

[28] H. Hellmers, A. Norrdine, J. Blankenbach, and A. Eichhorn, "An imu/magnetometer-based indoor positioning system using kalman filtering," in *IEEE Int. Conf. IPIN 2013*, Montbeliard-Belfort, France, 2003, DOI: 10.1109/IPIN.2013.6817887.

[29] J. A. Hesch, D. G. Kottas, S. L. Bowman, and S. I. Roumeliotis, "Camera-IMU-based localization: Observability analysis and consistency improvement," *Int. J. Robot. Research*, vol. 33, no. 1, pp. 182–201, 2014.

[30] T.-H. Hwang, J. Reh, A. Effenberg, and H. Blume, "Real-time gait event detection using a single head-worn inertial measurement unit," in *IEEE ICCE-Berlin 2016*, Berlin, Germany, 2016, pp. 28–32.

[31] J. Rueterbories, E. G. Spaich, B. Larsen, and O. K. Andersen, "Methods for gait event detection and analysis in ambulatory systems," *Med. Eng. & Physics*, vol. 32, no. 6, pp.545–552, Jul. 2010.
[32] R. Cromwell and R. Wellmon, "Sagittal plane head stabilization during level walking and ambulation on stairs," *Physiotherapy Res. Int.*, vol. 6, no. 3, pp. 179–192, Aug. 2001.
[33] J. J. Kavanagh, S. Morrison, and R. S. Barrett, "Coordination of head and trunk accelerations during walking," *European J. Applied Physiology*, vol. 94, no. 4, pp. 468–475, Apr. 2005.
[34] J. Kavanagh, R. Barrett, and S. Morrison, "The role of the neck and trunk in facilitating head stability during walking," *Experimental brain research*, vol. *172, no. 4*, pp. 454–463, Feb. 2006.
[35] E. Hirasaki, T. Kubo, S. Nozawa, S. Matano, and T. Matsunaga, "Analysis of head and body movements of elderly people during locomotion," *Acta Oto-Laryngologica*, Suppl. 501, pp. 25–30, 1993.
[36] D. Jarchi, C. Wong, R. M. Kwasnicki, B. Heller, G. A. Tew, and G. Z. Yang, "Gait parameter estimation from a miniaturized ear-worn sensor using singular spectrum analysis and longest common subsequence," *IEEE Trans. Biomed. Eng.*, vol. 61, no. 4, pp. 1261–1273, 2014.
[37] S. E. Bialkowski, "Real-time digital filters: Infinite-impulse response filters," *Analytical Chemistry*, vol. 60, no. 6, pp. 403A–413A, Mar. 1988, DOI: 10.1021/ac00157a003.
[38] S. E. Bialkowski, "Real-time digital filters: Finite-impulse response filters," *Analytical Chemistry*, vol. 60, no. 5, pp. 355A–361A, Mar. 1988, DOI: 10.1021/ac00156a743.
[39] D. Roetenberg, H. Luinge, and P. Slycke. "Xsens MVN: Full 6DOF human motion tracking using miniature inertial sensors," *Xsens Motion Technologies BV*, Tech. Rep. 1, Apr. 2009.
[40] S. Ghai, I. Ghai, G. Schmitz, and A. O. Effenberg, "Effect of rhythmic auditory cueing on parkinsonian gait: A systematic review and meta-analysis," *Scientific reports*, vol. 8, p. 506, Jan. 2018.
[41] A. O. Effenberg, U. Fehse, G. Schmitz, B. Krueger, and H. Mechling, "Movement sonification: Effects on motor learning beyond rhythmic adjustments," *Frontiers in Neuroscience*, vol. 10, p. 219, May 2016.

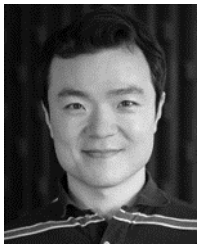

Tong-Hun Hwang (S'09, S'18) was born in Anyang, Korea, in 1982. He received the B.S. degree in electrical and computer engineering from the Hanyang University, Seoul, Korea, in 2008 and the M.S. degree in electronics and computer engineering from the same university in 2010. He is currently pursuing the Ph.D. degree in the Institute of Microelectronic Systems at Leibniz University Hannover, Germany.

From 2008 to 2010, he researched on transparent display panels with the Electronics and Telecommunications Research Institute (ETRI). He also researched on a capacitive touch panel system on a mobile display screen. From 2010 to 2013, he joined Multimedia Platform Group of the System LSI Division in Samsung Electronics. He was responsible for embedded software of image signal processor (ISP) that supports mobile camera applications. Since 2015, he is a research assistant with the Institute of Sport Sciences, Leibniz University Hannover, Germany. His research interest includes measurement systems of human movement, gait analysis, socializing sensorimotor contingency, health monitoring systems and home-based rehabilitation.

Julia Reh received the B.S. degree in Sport and Performance in 2011 and the M.S. degree in Sport Technology from the German Sport University Cologne in 2013.

During the master's program she joined the Sport Biomechanics Lab of the Cardiff Metropolitan University, Wales, United Kingdom from 2012 to 2013. Following her graduation, she was a research assistant with the Institute of Musculoskeletal Medicine, University Hospital Münster, in 2014. Since 2015, she has been a Research Associate with the Institute of Sport Sciences, Leibniz University Hanover, Germany. Her research interest includes movement sonification and gait analysis with a focus on the development of acoustic feedback systems for gait rehabilitation and its effect on gait symmetry after unilateral artificial joint replacement.

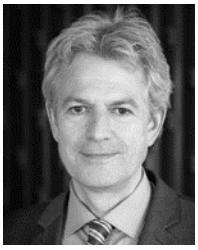

Alfred O. Effenberg was born in Hamburg. He received his Diplom (1991) and Ph.D. (1995) in Sport Science from the University of Hamburg.

In 1993, he was a visiting researcher at UCLA with Prof. Richard A. Schmidt. From 1995 to 2002, he was a postdoctoral researcher and successfully finished his postdoctoral lecture qualification at the University of Bonn in 2002. Since 2007, he is a professor and the head of Institute of Sports Science and the Science in Motion Research Group at the Leibniz University Hannover. He has published more than 130 papers - including 46 in peer-reviewed journals and conferences - as well as book chapters and books. He organized the international dvs-conference "Multisensory Motor Behavior: Impact of Sound," 2013, Hannover, Germany together with ETH/Zurich. His main research interests are located in the fields of multisensory integration, motor perception, control and learning. He established the movement sonification approach with current research projects of BMBF, BMWi and EU HORIZON 2020.

Holger Blume (M'98–SM'12) received his diploma in electrical engineering in 1992 at the University of Dortmund, Germany. In 1997 he achieved his Ph.D. with distinction from the University of Dortmund, Germany.

Until 2008, he worked as a senior engineer and as an academic senior counselor at the Chair of Electrical Engineering and Computer Systems (EECS) of the RWTH Aachen University. In 2008, he got his postdoctoral lecture qualification. He has been professor for "Architectures and Systems" at the Leibniz University Hannover, Germany, since July 2008 and manages the Institute for Microelectronic Systems. His present research includes algorithms and heterogeneous architectures for digital signal processing, design space exploration for such architectures as well as research on the corresponding modeling techniques.

Prof. Blume is IEEE Senior Member and since 2000 chairman of the German chapter of the IEEE Solid State Circuits Society (SSCS). He is in the steering committee of the annual SAMOS (Systems, Architectures, Modeling and Simulation) Conference as a program chairman (2007) and as a general chair (2008). He is also a member of the German Institute of Information Technology Engineers (ITG of VDE)